

Cross-Linkable Polyspirobifluorenes: A Material Class Featuring Good OLED Performance and Low Amplified Spontaneous Emission Thresholds

Bodo H. Wallikewitz, Dirk Hertel, and Klaus Meerholz*

Chemistry Department, University of Cologne, Luxemburger Str. 116, 50939 Cologne, Germany

Received February 27, 2009. Revised Manuscript Received May 4, 2009

We report on an in-depth study of cross-linkable polyspirobifluorene (PSF) copolymers for organic lasing applications. We investigate the performance of the materials in organic light-emitting diodes (OLED) and the optically pumped amplified spontaneous emission (ASE) properties of the new PSF-based devices. The influence of chemical composition and cross-linking of the copolymers is investigated. The cross-linkable polymers presented here exhibit low ASE thresholds and simultaneously good OLED efficiencies. This is exceptional, as we demonstrate that usually only one of these properties is optimized in semiconducting polymers. The ASE threshold in the green-emitting materials is as low as $4.4 \mu\text{J}/\text{cm}^2$ under nanosecond excitation. The chemical cross-linking of the polymers into an insoluble network has little effect on the ASE properties. With the material exhibiting the best figure-of-merit we fabricated a slab-waveguide OLED. This OLED exhibits a low, almost preserved ASE threshold compared to a single layer on glass and concomitantly good luminescence efficiency. Overall, the use of these materials in future organic laser diodes seems promising.

I. Introduction

The tremendous improvement in performance of organic light emitting diodes (OLEDs) in the past decade^{1–4} has stimulated intense research for the realization of more challenging devices such as laser diodes.^{5,6} A prerequisite for laser operation is optical gain, that is, stimulated emission, in the emitting material. With conventional laser dyes such as DCM (4-dicyanomethylene-2-methyl-6-*p*-dimethylamino-styryl-4*H*-pyran) used in small molecular OLEDs, stimulated emission has been demonstrated for the solid state in a variety of materials.^{7–9} Optical gain in conjugated polymers has been reported first for

PPV-type materials by means of fs pump–probe spectroscopy.¹⁰ Meanwhile optical gain has frequently been observed in π -conjugated polymers such as methyl-substituted ladder-type poly(*p*-phenylene) (MeLPPP), poly(*p*-phenylene-vinylene)s (PPVs), and polyfluorene derivatives.^{11–17} The lowest threshold for amplified spontaneous emission (ASE) in solution-processable materials is $20 \text{ nJ}/\text{cm}^2$ reported by Lee et al.¹⁸ for a blend of PVK with a fluorene–phenylenevinylene copolymer. This low ASE threshold has been achieved with subnanosecond laser excitation. Common to most of the polymers with the currently best ASE properties is a rather poor performance in OLEDs (for example, MeLPPP and MEH-PPV). Naturally, combination of excellent ASE and OLED properties in one material is essential for eventually realizing an electrically pumped organic laser (OLAS). Despite of this, in most cases

*Corresponding author. E-mail: klaus.meerholz@uni-koeln.de.

- (1) Forrest, S. R. *Nature* **2004**, *428*, 911.
- (2) Friend, R. H.; Gymer, R. W.; Holmes, A. B.; Burroughes, J. H.; Marks, R. N.; Taliani, C.; Bradley, D. D. C.; Dos Santos, D. A.; Bredas, J. L.; Logdlund, M.; Salaneck, W. R. *Nature* **1999**, *397*, 121.
- (3) He, G.; Pfeiffer, M.; Leo, K.; Hofmann, M.; Birnstock, J.; Pudziel, R.; Salbeck, J. *Appl. Phys. Lett.* **2004**, *85*, 3911.
- (4) Organic Light Emitting Devices Synthesis, Properties and Applications; Müllen, K.; Scherf, U., Eds.; Wiley-VCH: Weinheim, Germany, 2006.
- (5) Scherf, U.; Riechel, S.; Lemmer, U.; Mahrt, R. F. *Curr. Opin. Solid State Mater. Sci.* **2001**, *5*, 143.
- (6) Schneider, D.; Lemmer, U.; Kowalski, W.; Riedl, T. In Organic Light Emitting Devices Synthesis, Properties and Applications; Müllen, K.; Scherf, U., Eds.; Wiley-VCH: Weinheim, Germany, 2006; p 369.
- (7) Bulovic, V.; Kozlov, V. G.; Khalifin, V. B.; Forrest, S. R. *Science* **1998**, *279*, 553.
- (8) Berggren, M.; Dodabalapur, A.; Slusher, R. E.; Bao, Z. *Nature* **1997**, *389*, 466.
- (9) Aimono, T.; Kawamura, Y.; Goushi, K.; Yamamoto, H.; Sasabe, H.; Adachi, C. *Appl. Phys. Lett.* **2005**, *86*, 071110.
- (10) Yan, M.; Rothberg, L. J.; Papadimitrakopoulos, F.; Galvin, M. E.; Miller, T. M. *Phys. Rev. Lett.* **1994**, *72*, 1104.

- (11) Haugeneder, A.; Hilmer, M.; Kallinger, C.; Perner, M.; Spirkl, W.; Lemmer, U.; Feldmann, J.; Scherf, U. *Appl. Phys. B-Lasers Opt.* **1998**, *66*, 389.
- (12) McGehee, M. D.; Gupta, R.; Veenstra, S.; Miller, E. K.; Diaz-Garcia, M. A.; Heeger, A. J. *Phys. Rev. B* **1998**, *58*, 7035.
- (13) Heliotis, G.; Bradley, D. D. C.; Turnbull, G. A.; Samuel, I. D. W. *Appl. Phys. Lett.* **2002**, *81*, 415.
- (14) Laquai, F.; Mishra, A. K.; Ribas, M. R.; Petrozza, A.; Jacob, J.; Akcelrud, L.; Müllen, K.; Friend, R. H.; Wegner, G. *Adv. Funct. Mater.* **2007**, *17*, 3240.
- (15) Xia, R. D.; Heliotis, G.; Hou, Y.; Bradley, D. D. C. *Org. Electron.* **2003**, *4*, 165.
- (16) Laquai, F.; Mishra, A. K.; Müllen, K.; Friend, R. H. *Adv. Funct. Mater.* **2008**, *20*, 3265.
- (17) Yap, B. K.; Xia, R.; Campoy-Quiles, M.; Stavrinou, P. N.; Bradley, D. D. C. *Nat. Mat.* **2008**, *7*, 376.
- (18) Lee, T.-W.; Choi, O. O. H.; Cho, H. N.; Kim, Y. C. *Appl. Phys. Lett.* **2002**, *81*, 424.

reported in the literature either the optical (ASE, gain) or the electrical (OLED at high current densities) properties are studied without paying attention to the other property necessary to achieve electrically pumped lasing. Only in the case of two small-molecule systems have both optical and electrical investigations been reported.^{19,20} By contrast, for polymeric systems such comprehensive study is still missing due to the lack of suitable materials.

OLEDs operate in a low-current-density regime as opposed to potential laser diodes. Unfortunately, there is little experimental knowledge about relevant processes under high-current-density driving which would be necessary to reach lasing threshold. Baldo and co-workers²¹ have addressed this issue with focus on low-molecular-weight materials. They concluded that the efficiency needed to be improved and that a potential organic laser has to be a multilayer device.²² Recently, we have shown that the use of oxetane-functionalized cross-linkable conjugated polymers allows the fabrication of OLEDs with exceptional performance.^{23,24} These polymers can not only be structured for display applications²⁵ but also be used to fabricate multilayer devices.^{26–28} These enable the construction of slab-waveguide devices, enabling low ASE thresholds in the presence of electrodes, mandatory for future electrically driven organic lasers.²⁹ Finally, cross-linked materials do not soften, which could be an important advantage under very high current drive conditions, where temperatures in excess of 100 °C can easily be attained.

In this study, we investigate the suitability of cross-linkable polyspirofluorene (PSF) copolymers as gain media for lasing. These materials can be cross-linked photochemically in the presence of a photoinitiator by cationic ring-opening polymerization (CROP).²⁴ Furthermore, for comparison we have included in our study one of the best (in terms of lifetime and electrical current it can withstand) OLED materials, the PPV-based “Super Yellow” (SY) exhibiting high efficiency and excellent long-term stability, as well as MeLPPP,^{5,6,16} exhibiting one

of the lowest ASE thresholds for solution-processed polymeric materials reported so far.

We have performed ASE measurements using the well established stripe length method,^{12,13} studying in detail the dependence of the ASE threshold on the chemical composition of the polymers (chemical nature of the emissive chromophore and its content) and the influence of the cross-linking process. We demonstrate that these polymers exhibit high optical gain and low losses. We then evaluate all materials in standard single-layer OLEDs to determine the PSF polymer with the best optical and electrical properties. Finally, this PSF polymer is incorporated in a multilayer OLED where thick charge-transport layers are cladding the cross-linked polymer emitter layer to minimize waveguide losses. This device exhibits good OLED performance and still almost unchanged ASE characteristics compared to a simple film on glass.

II. Experimental Section

Details about the synthesis of the polymers used in this study have been reported previously.²³ The chemical structures of the monomer components constituting the PSF polymers are depicted in Scheme 1. The chemical composition is listed in Table 1. Common to all polymers are monomer units of spirobifluorene (**1**), a fluorene unit (**2** or **3**), a tetraphenylene-diamine (TPD) as hole transporting unit (**4**), and green- (**5**, **6**, or **7**) or red-emitting chromophores (**8** and **9**). We will refer to the polymers by stating the emission color (B, G, and R, respectively) and the monomer number, followed by the chromophore content in parentheses. An “X” will be added, whenever the polymer is cross-linkable. For example, the polymer **XG5(15)** will be a cross-linkable green-emitting polymer, containing 15% of the monomer **5**.

All samples were fabricated under inert nitrogen atmosphere. Polymer films were prepared either on cleaned quartz substrates or Si wafers with a 600 nm thermally oxidized SiO_x layer by spin coating from toluene solution (8 g/L). For the **XG6(25)** a concentration of 24 g/L was used. X-HTLs and ETLs were spin-coated from 50 g/L or 20 g/L toluene solution, respectively. The film thickness was measured with a Dektak 3 surface profilometer.

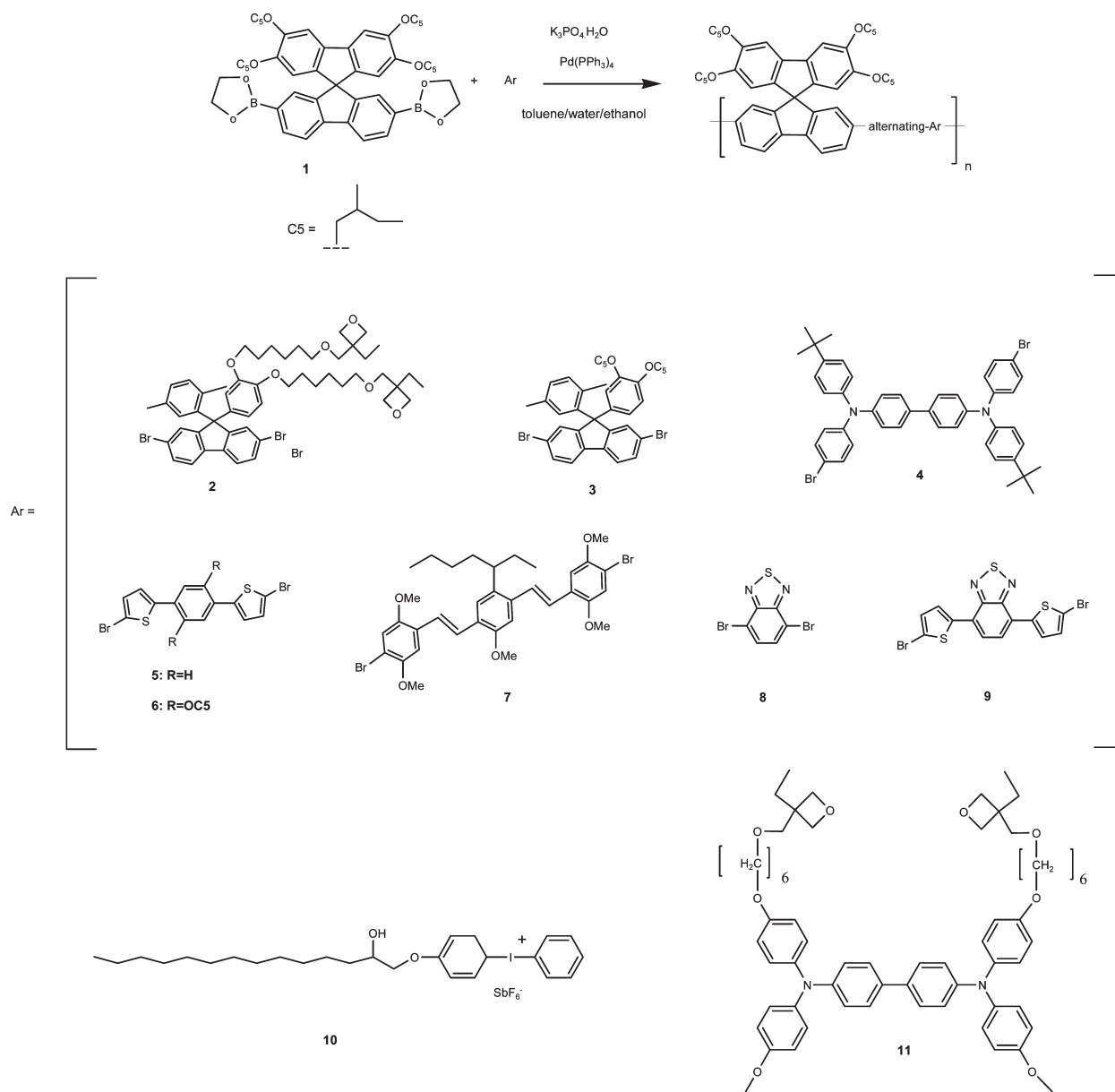
To obtain insoluble polymer layers, photoinduced cationic ring-opening polymerization (CROP) of the oxetane side groups has been performed; therefore, the photoacid {4-[(2-hydroxytetradecyl)-oxyl]-phenyl}-phenyliodonium hexafluoroantimonate (OPPI, Aldrich) dissolved in toluene was added. The concentration of OPPI was 0.5 or 1% by weight of polymer. After mixing, spin coating was performed under red light illumination. The resulting films were irradiated with 366 nm light for 10 s and cured at 100 °C for 1 min. Thorough rinsing of the polymer layer with toluene followed by a baking step at 150 or 200 °C for 1 min completed the procedure.

Absorption spectra were measured with a Cary 50 Bio (Varian) UV/vis spectrometer. Fluorescence excitation spectra were recorded on a Varian Eclipse and corrected for the spectral response of the excitation monochromator by using Rhodamin B as a quantum counter.³⁰

OLEDs of the polymers were fabricated on ITO substrates covered with 20 nm PEDOT:PSS (Clevios AL 4083, H.C. Starck

- (19) Matsushima, T.; Adachi, C. *Jpn. J. Appl. Phys.* **2007**, *46*, L861.
- (20) Yamamoto, H.; Oyamada, T.; Sasabe, H.; Adachi, C. *Appl. Phys. Lett.* **2004**, *84*, 1401.
- (21) Baldo, M. A.; Holmes, R. J.; Forrest, S. R. *Phys. Rev. B* **2002**, *66*, 035321.
- (22) Gärtner, C.; Karnutsch, C.; Lemmer, U.; Pflumm, C. *J. Appl. Phys.* **2007**, *101*, 023107.
- (23) Müller, D. C.; Falcou, A.; Reckefuss, N.; Rohjan, M.; Wiederhirn, V.; Rudati, P.; Frohne, H.; Nuyken, O.; Becker, H.; Meerholz, K. *Nature* **2003**, *421*, 829.
- (24) Meerholz, K.; Müller, D. C.; Nuyken, O. In *Organic Light Emitting Devices Synthesis, Properties and Applications*; Müllen, K.; Scherf, U., Eds.; Wiley-VCH: Weinheim, Germany, 2006; p 293.
- (25) Gather, M. C.; Köhnen, A.; Falcou, A.; Becker, H.; Meerholz, K. *Adv. Funct. Mater.* **2006**, *17*, 191.
- (26) Müller, D. C.; Braig, T.; Nothofer, H.-G.; Arnoldi, M.; Gross, M.; Scherf, U.; Nuyken, O.; Meerholz, K. *ChemPhysChem* **2000**, *1*, 207.
- (27) Köhnen, A.; Gather, M. C.; Riegel, N.; Zacharias, P.; Meerholz, K. *Appl. Phys. Lett.* **2007**, *91*, 119501.
- (28) Zacharias, P.; Gather, M. C.; Rojan, M.; Nuyken, O.; Meerholz, K. *Angew. Chem., Int. Ed.* **2007**, *46*, 4388.
- (29) Reufer, M.; Feldmann, J.; Rudati, P.; Ruhl, A.; Müller, D.; Meerholz, K.; Karnutsch, C.; Gerken, M.; Lemmer, U. *Appl. Phys. Lett.* **2005**, *86*, 221102.

- (30) Lakowicz, J. R.; *Principles of Fluorescence Spectroscopy*; Kluwer Academic: Dordrecht, 1999.

Scheme 1. Sketch of the Synthetic Route (Suzuki Coupling) to the Studied Polymers and Chemical Structures of the Monomers Used for Polymerization^a


^aThe chemical structures of the photo-initiator OPPI **10** and the cross-linkable hole transport layer X-HTL **11** are also shown.

GmbH). For cross-linking the above-described procedure was applied. Ba and Ag were evaporated as cathode at a pressure of 10^{-6} mbar through a shadow mask. Luminance–current–voltage characteristics were measured using a Keithley 2400 source meter and a calibrated photodiode.

For ASE measurements the samples were placed in a nitrogen flow cryostat (Cryovac) and measured at room temperature. Photoluminescence (PL) was excited with a Nd:YAG (Surelite I, Continuum) pumped dye laser (NARROWscan, Radiant Dyes) operated at a repetition rate of 10 Hz. The pulse duration is 5 ns. The excitation intensity was varied by neutral density filters and measured simultaneously with a thermoelectric detector (Sciencetech). A cylindrical lens ($f = 200$ mm) was used to focus the laser beam to a $4 \text{ mm} \times 0.1 \text{ mm}$ (fwhm) stripe incident normal to the film surface. To obtain a Gaussian laser profile for excitation a telescope and appropriate slits were used. The beam profile was controlled for each measurement using an imaging

CCD (WinCam D, Gentec). The PL was collected from the edge of the film, focused onto the entrance slit of the monochromator, and detected by an intensified CCD camera (PI-MAX II, Roper Scientific). Three different gratings in the monochromator (Spectra Pro 2300i, Acton) allowed for varying resolution depending on the required accuracy. Typical PL spectra were averaged over 100 laser pulses.

To obtain quantitative information about the optical gain we have measured the ASE intensity as a function of excitation stripe length and excitation intensity. The output intensity I depends exponentially on the gain g and stripe length l according to¹²

$$I(\lambda) = \frac{A(\lambda)I_0}{g(\lambda)} (e^{g(\lambda)l} - 1) \quad (1)$$

Here, I_0 is the excitation intensity and A is related to the stimulated emission cross section. Fitting the measured data

Table 1. Composition and Physical Properties of the EL Polymers Investigated in Our Study^a

polymer name	backbone (blue)				green chromophores			Red Chrom.		λ_{\max} abs [nm]	λ_{\max} PL [nm]
	M1	M2	M3	M4	M5	M6	M7	M8	M9		
B	50	0	40	10	0	0	0	0	0	397	454
XB	50	25	15	10	0	0	0	0	0	399	457
G5(10)	50	0	30	10	10	0	0	0	0	390	485
G5(20)	50	0	20	10	20	0	0	0	0	398	490
G5(30)	50	0	10	10	30	0	0	0	0	412	492
XG5(15)	50	15	10	10	15	0	0	0	0	394	488
G6(25)	50	0	15	10	0	25	0	0	0	403	508
XG6(25)	50	15	0	10	0	25	0	0	0	404	509
XG7(15)	50	25	0	10	0	0	15	0	0	392	507
R	50	0	25	10	0	0	0	10	5	393	650
XR	50	10	15	10	0	0	0	10	5	394	650
MeLPPP										455	464
F8BT										460	550
SY										443	598

^aThe monomers **M1** through **M9** are listed following Scheme 1. λ_{\max} abs and λ_{\max} PL are the maximum wavelengths of absorption and photoluminescence, respectively.

enables calculation of the gain. Least square fitting has been used, taking into account only values below saturation. The error introduced upon fitting is smaller than sample to sample variations.

To estimate the waveguide losses an excitation stripe of fixed area ($0.4 \times 0.01 \text{ cm}^2$) is shifted relative to the edge of the film. The emission is measured as a function of stripe position and can be calculated according to

$$\ln \frac{I}{I_0} = -\alpha l \quad (2)$$

where I and I_0 are the output intensity emitted from the edge and the pump intensity, respectively, α is the absorption coefficient, and l is the distance from the edge.

III. Results and Discussion

Absorption and Emission Spectra. Figure 1 shows the absorption and fluorescence spectra of representative examples of the investigated PSF polymers. The absorption of **G5(10)** (dotted line) is characterized by a broad band with a maximum at 390 nm (3.18 eV) corresponding to the $\pi-\pi^*$ transition of the polymer backbone. The long tail at the low energy side of the spectrum extends to about 480 nm and is characteristic of the chromophore absorption; that is, it increases with increasing chromophore content and becomes most pronounced for **G5(30)** as a shoulder at 465 nm (Figure 1). Correspondingly the absorption maximum shifts from 390 nm for **G5(10)** to 412 nm for **G5(30)**. The absorption spectra of cross-linked and not cross-linked **XG6(25)** are virtually identical to the spectra of **G5(20)** except for the slight red-shift of the absorption tail.

The fluorescence of all PSF polymers is characterized by the $S_1 \rightarrow S_0(0-0)$ transition around 490 nm (2.53 eV) with a vibronic splitting of about 170 meV (Figure 1). If the amount of chromophore is varied from 10% (**G5(10)**) to 30% (**G5(30)**) the $S_1 \rightarrow S_0(0-0)$ transition is shifted from 485 nm (2.55 eV) to 492 nm (2.52 eV) (Table 1). The vibronic splitting remains almost constant. The red shift in emission can be explained by an increase in efficiency of energy transfer with increasing chromophore content.

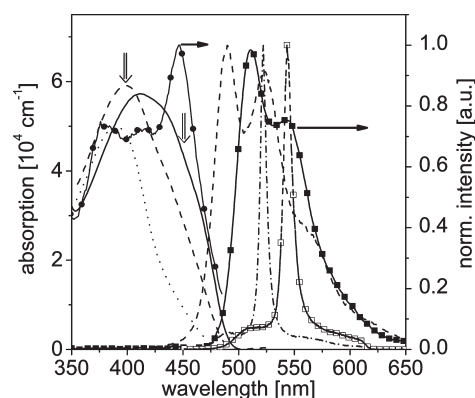


Figure 1. Normalized absorption spectra of **G5(10)** (dotted line), **G5(20)** (dashed line), and **G5(30)** (solid line). The vertical arrows indicate the excitation wavelength for ASE measurements at 398 and 450 nm. The solid line with circles is the fluorescence excitation spectrum of **G5(30)**. The dashed line on the right shows the normalized fluorescence spectrum of **G5(20)**. The dashed/dotted line shows the normalized ASE spectrum of **G5(20)**. The dashed line with open squares shows the normalized ASE spectrum of **XG6(25)** (at $E = 2.5E_{\text{th}}$). The solid line with solid squares shows the normalized EL spectrum from the slab-waveguide OLED based on **XG6(25)** at a current density of 30 mA/cm^2 (similar for other currents).

ASE Properties. To study the optical gain properties of our PSF polymers we have used ASE measurements at different excitation intensities and excitation wavelengths. In order to obtain ASE we have used the well-known stripe-length method,^{12,13} where the polymer film is excited with a rectangular laser spot and the photoluminescence (PL) emission is detected from the edge of the sample. If one measures the PL as a function of pump intensity, ASE is manifested by spectral narrowing at the maximum gain wavelength. In Figure 1 the emission spectrum well above ASE threshold ($\sim 2.5E_{\text{th}}$) is presented for **G5(20)** and **XG6(25)**. An excitation wavelength of 450 nm has been used to excite the chromophore directly. The peak position of ASE is 522 nm for **G5(20)** (Table 1) and coincides with the $S_1 \rightarrow S_0(0-1)$ transition. This is common for organic materials where the low energy absorption tail overlaps with the high energy side of the fluorescence spectrum and concomitantly reduces the optical gain^{5,6} at the $S_1 \rightarrow S_0(0-0)$ transition.

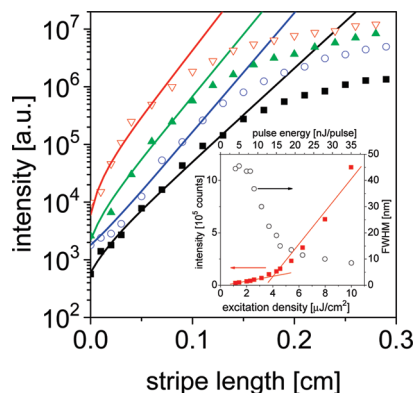


Figure 2. Dependence of the intensity at the ASE peak of **G5(30)** on excitation stripe length. The excitation density has been varied from $35 \mu\text{J}/\text{cm}^2$ (solid squares), $50 \mu\text{J}/\text{cm}^2$ (open circles), and $75 \mu\text{J}/\text{cm}^2$ (solid triangles) to $100 \mu\text{J}/\text{cm}^2$ (open triangles). The data are offset for clarity. The lines are fits to the data according to eq 2 (see Section II for details). The inset depicts the PL output (solid squares) at 517.6 nm as a function of excitation density for **G5(10)** (left scale). The inflection points of the tangents correspond to an ASE threshold of $4.4 \mu\text{J}/\text{cm}^2$ ($14 \text{ nJ}/\text{pulse}$). The decrease of the width of the ASE band (full width at half-maximum (fwhm)) with increasing excitation density is shown as well (open circles).

As observed already in the fluorescence spectra, the ASE peak position shifts to lower energy with increasing chromophore content but remains in line with the $S_1 \rightarrow S_0$ ($0-1$) transition (see Table 1). As in the fluorescence spectra, cross-linking has no noticeable effect on the ASE spectra.

Having established that the spectral narrowing is due to the occurrence of ASE, we are able to determine its threshold. In the inset of Figure 2 the PL intensity at the ASE peak wavelength for **G5(10)** is plotted as a function of pump intensity. For low pump fluence the PL increases linearly with excitation intensity, whereas at higher pump intensity a superlinear increase is observed. The ASE threshold as obtained from the crossing of two tangents on the different regimes amounts to $4.4 \mu\text{J}/\text{cm}^2$ or $12 \text{ nJ}/\text{pulse}$. At the same excitation intensity the $S_1 \rightarrow S_0$ ($0-1$) transition narrows from 45 nm fwhm at low intensity to $< 10 \text{ nm}$ for high pump intensity. If we would use the excitation spot size at the $1/e^2$ value to calculate the excitation density and use the method described in ref 31 our ASE threshold would be $0.7 \mu\text{J}/\text{cm}^2$.

Similar results have been obtained for all other polymers investigated in this study, and the results are compiled in Table 2. Clearly, all green-emissive PSF polymers show much lower ASE thresholds as compared to the red- and blue-emissive materials. The lowest ASE threshold is obtained for the polymer **G5(10)**. With increasing chromophore content the ASE threshold increases slightly for a given excitation wavelength. The loss in performance is probably due to nonradiative decay if one excites higher lying singlet states of the chromophore or excitation transfer to quenching sites occurs. Apparently, at 398 nm one excites not only higher lying states of the chromophore but also a large amount of subunits of the polymer backbone. From these segments the excitation

has to migrate by Förster transfer to the chromophore to contribute to emission.³² This hypothesis is validated by the fluorescence excitation spectra, which are a measure of the relative fluorescence quantum yield. Characteristic for the excitation spectra of our polymers is the decrease of fluorescence for excitation of the polymer backbone, that is, below $\sim 450 \text{ nm}$, shown for **G5(30)** in Figure 1 (filled circles). This excludes other sources for the loss such as singlet–singlet annihilation which becomes significant only at excitation intensities about 1 order of magnitude higher than the ASE threshold.

Introduction of the oxetane-containing monomer **2** (which replaces monomer **3**; see Table 1) increases the ASE threshold by about 15–20% for an excitation wavelength of 450 nm (Table 2). Furthermore, cross-linking has little or no effect on the ASE threshold.

Comparison of our results with literature data of other polymer-based devices can only be obtained for similar experimental conditions. The temporal length of the excitation pulse has a strong influence on the ASE threshold, because the time scale of ASE and energy transfer are comparable.^{5,6,33} As long as the excitation pulse is shorter than the fluorescence lifetime, the ASE threshold decreases with decreasing pulse length. Bauer et al.³⁴ described a decrease of the threshold by 2 orders of magnitude using femtosecond excitations compared to nanosecond excitations. In our experiments the pulse length (4 ns) is comparable or longer than excited state lifetime; therefore, we expect a significant decrease of the ASE threshold under femtosecond³⁴ or picosecond^{18,31} excitation conditions.

Also for excitation pulse length in the range of ps low ASE thresholds of $0.8 \mu\text{J}/\text{cm}^2$ ³¹ and $0.02 \mu\text{J}/\text{cm}^2$ ¹⁸ have been reported. Unfortunately, it is unclear whether the fwhm or the $1/e^2$ value of the excitation spot has been used to calculate the excitation density. This can result in a decrease of the threshold value by a factor of 3. Furthermore, a double logarithmic fwhm vs. energy density plot presented in ref 31 is more sensitive to spectral changes of the PL and, thus, results in a decrease of the threshold compared to a linear PL intensity vs energy density plot, like used in this work.

Low ASE threshold of $< 1 \mu\text{J}/\text{cm}^2$ has been reported for the blue spectral range.¹⁸ However, no electrical data is reported for this material. Our green-emitting PSF polymers exhibit slightly higher ASE thresholds. Nevertheless, these are among the lowest thresholds for green emitting polymers reported so far.^{12,13,15} Under our experimental conditions the ASE threshold of the blue emitting MeLPPP is $12 \mu\text{J}/\text{cm}^2$ and approximately $5 \mu\text{J}/\text{cm}^2$ for PFO.³⁵ The ASE threshold of the green

(31) Görrn, P.; Rabe, T.; Riedl, T.; Kowalsky, W.; Galbrecht, F.; Scherf, U. *Appl. Phys. Lett.* **2006**, *89*, 161113.

(32) Vehse, M.; Liu, B.; Edman, L.; Bazan, G. C.; Heeger, A. J. *Adv. Mater.* **2004**, *16*, 1001.

(33) Wegmann, G.; Schweitzer, B.; Hertel, D.; Giessen, H.; Oestreich, M.; Scherf, U.; Müllen, K.; Mahrt, R. F. *Chem. Phys. Lett.* **1999**, *312*, 376.

(34) Bauer, C.; Giessen, H.; Schnabel, B.; Kley, E.-B.; Schmitt, C.; Scherf, U.; Mahrt, R. F. *Adv. Mater.* **2001**, *13*, 1161.

(35) Ryu, G.; Xia, R.; Bradley, D. D. C. *J. Phys.: Condens. Matter* **2007**, *19*, 056205.

Table 2. E_{th} , FWHM, λ_{max} , gain, d , η_{max} , $\lambda_{\text{max,EL}}$, and FOM^a

polymer name	$\langle E_{\text{th}} \rangle$ (450 nm) [$\mu\text{J}/\text{cm}^2$]	$\langle E_{\text{th}} \rangle$ (398 nm) [$\mu\text{J}/\text{cm}^2$]	fwhm ASE peak [nm]	λ_{ASE} [nm]	gain [cm^{-1}]	d [nm]	η_{max} [cd/A]	$\lambda_{\text{max,EL}}$ [nm] (ECF)	FOM
XB		3.7×10^3		457.0	0	105	3.0	454 (0.05)	0
XB cross-linked		3.7×10^3		457.0	0	105	3.0	457 (0.05)	0
G5(10)	4.4 ± 0.6	7.7 ± 0.3	5.5	517.6	39.5	114	6.5	485 (0.17)	8.7
G5(20)	5.3 ± 0.6	8.5 ± 0.8	6.0	522.0		107	6.7	489 (0.20)	6.3
G5(30)	5.5 ± 0.7	8.8 ± 1	5.2	526.7	53.0	122	7.6	492 (0.23)	6.0
XG5(15)	6.1 ± 0.1	9.6 ± 0.3	6.0	520.0	37.0	100	6.2	488 (0.19)	5.4
XG5(15) cross-linked	6.6 ± 0.5	10 ± 1	7.2	520.5	40.0	104	3.3	488 (0.19)	2.6
G6(25)	6.0 ± 0.6	11 ± 1	7.0	543.0		122	9.0	508 (0.46)	3.3
XG6(25)	7.0 ± 1.0	13 ± 1	5.0	544.0		250	9.1	509 (0.48)	2.7
XG6(25) cross-linked	7.0 ± 1.0	13 ± 1	6.0	543.0		250	6.2	509 (0.48)	1.9
XG7(15)	10.0 ± 1.0			538.0		120	7.0	507 (0.45)	1.6
XG7(15) cross-linked	10.0 ± 1.0			538.0		120	6.5	507 (0.45)	1.4
XR		1.4×10^3		650.0	0	161	1.1	650 (0.11)	0
XR cross-linked		1.4×10^3		650.0	0	161	1.1	650 (0.11)	0
MeLPPP	12 ± 1.5			493.0	16^{16}	115	0.2	466 (0.08)	0.2
F8BT	28^{15b}				22^{15}		2.0^{46}	555^{46} (1)	0.07
SY		100 ± 5		588.0	0	120	11.6	585 (0.82)	0

^a E_{th} gives the ASE threshold obtained at 450 and 398 nm, respectively. FWHM is the full width at half maximum of the ASE band, and λ_{max} is the wavelength of the ASE peak. The optical gain at an excitation density of $100 \mu\text{J}/\text{cm}^2$, the film thickness d , and the maximum luminous efficiency η_{max} of the OLEDs are also listed. ^b Excitation at 440 nm.

emitting polyfluorene F8BT is $28 \mu\text{J}/\text{cm}^2$,¹⁵ measured under similar conditions. These thresholds are up to five times higher than the threshold in the best PSF polymer (Table 2). The ASE threshold of SY is only detectable by a slight spectral change in the PL spectra and can be estimated to be $\sim 100 \mu\text{J}/\text{cm}^2$.

Optical Gain. In Figure 2 the ASE intensity of **G5(30)** is plotted as a function of excitation stripe length for four different excitation densities. Upon increasing the stripe length the output intensity increases exponentially as expected and saturates for stripe length of about 0.3 cm for the lowest pump intensity of $35 \mu\text{J}/\text{cm}^2$. The saturation stripe length decreases by a factor of 2 as the pump intensity is increased to $100 \mu\text{J}/\text{cm}^2$. From fitting the data a net gain (i.e., already including absorption losses) of 53 cm^{-1} for **G5(30)** is calculated at an excitation density of $100 \mu\text{J}/\text{cm}^2$. (For details of the gain and loss calculations see Section II). This has to be compared to F8BT, another fluorene-based polymer, for which an optical net gain of 22 cm^{-1} has been determined under similar experimental conditions, but for six times higher excitation densities.¹⁵ Furthermore, for a green-emitting PPV derivative a higher gain value (62 cm^{-1}) has been reported¹² but it concomitantly exhibits an order of magnitude higher losses of 44 cm^{-1} . The dependence of the gain at the ASE peak maximum on the excitation density is plotted in Figure 3 for **G5(10)**, **G5(30)**, and **XG5(15)**. At low excitation density, the gain first increases linearly and then saturates for all polymers above $100 \mu\text{J}/\text{cm}^2$. Since this behavior is largely independent of the chromophore concentration, the gain saturation at large excitation densities cannot be due to saturation of absorption. A possible reason is singlet–singlet annihilation (SSA), which becomes significant above $30 \mu\text{J}/\text{cm}^2$ as verified by intensity-dependent PL measurements (not shown). The high net gain of the materials is accompanied by low optical losses. Within experimental error the losses are $3 \pm 1 \text{ cm}^{-1}$, independent of excitation intensity (Figure 3).

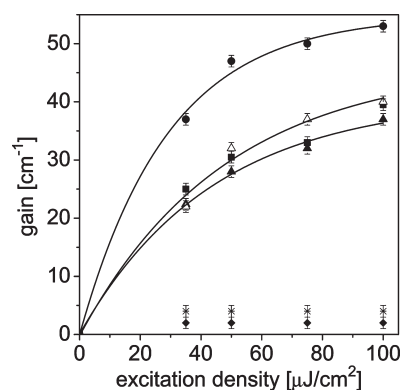


Figure 3. Dependence of the optical gain at the wavelength of the ASE peak maximum on the excitation density for **G5(10)** (solid squares), **XG5(15)** (open triangles), cross-linked **XG5(15)** (solid triangles), and **G5(30)** (solid circle). For **G5(10)**, **G5(30)** (star), and cross-linked **XG5(15)** (diamonds) the optical losses are shown as well. The lines are a guide to the eye. The error bars reflect sample-to-sample variations.

For the materials XR, XB, and SY, no optical gain could be determined.

OLED Performance. To evaluate the potential of PSF polymers in terms of electrical driving we have fabricated simple single-layer OLEDs of the general structure ITO/PEDOT:PSS(20 nm)/PSF(80 nm)/Ba(4 nm)/Ag(100 nm). Within the series of PSF polymers, **G5(30)** has the highest efficiency (7.6 cd/A). This compares to 20 cd/A reported for green-emitting fluorescent OLED,³⁶ where poly(*p*-phenylen-vinylene) is used as active material.

With decreasing chromophore content, the efficiency drops from 7.6 cd/A (**G5(30)**) over 6.65 cd/A (**G5(20)**) to 6.5 cd/A for **G5(10)**. We explain this finding by the trapping of electrons on the chromophore.³⁷ Thus, a higher chromophore content increases the probability of recombination, therefore, leading to a higher probability

(36) Ho, P. K. H.; Kim, J. S.; Burroughes, J. H.; Becker, H.; Li, S. F. Y.; Brown, T. M.; Cacialli, F.; Friend, R. H. *Nature* **2000**, *404*, 481.

(37) Gather, M. C.; Alle, R.; Becker, H.; Meerholz, K. *Adv. Mater.* **2007**, *19*, 4460.

of emission. For the PSF polymers the peak efficiency is reached at lower voltage with increasing chromophore content (not shown). This indicates a higher charge injection efficiency with higher chromophore content. Both effects would be beneficial for the OLED efficiency.

Actual cross-linking of the cross-linkable PSF polymers may, in the best case, leave the OLED efficiency unaffected (XB and XR), but for the green-emitting polymers losses from 8% (XG7(15)) up to 50% (XG5(15)) have been observed. This indicates that the efficiency reduction due to cross-linking can be minimized by optimizing the chromophore structure.

The reference OLEDs based on SY reach efficiencies of 11.6 cd/A (Table 2) in agreement with literature data.³⁸ In contrast to the good ASE properties of MeLPPP, the efficiency of OLEDs based on this material is rather limited (0.2 cd/A). This compares with state-of-the-art blue-emitting polymer OLEDs with efficiencies of 3–4 cd/A.^{23,39}

Figure-of-Merit for Potential Laser Materials. In the following, we summarize the results from the previous sections to motivate the choice of the optimal PSF laser medium for application in future electrically pumped organic laser devices (OLAS). The higher the OLED efficiency and the smaller the ASE threshold, the better a material is suited for this application. Please note that a direct comparison of the luminous efficiencies (in [cd/A]) of materials emitting at different wavelengths is somewhat questionable. At shorter wavelengths (e.g., blue emitters such as MeLPPP) the eye sensitivity, which is included in the unit “candela”, is lower as compared to green emitters (such as our PSF polymers), which emit close to the maximum eye sensitivity. Therefore, we use an eye-correction factor (ECF < 1) to correct the OLED efficiency. As a zero-order approximation, we use the ECF for the maximum emission wavelength of the OLED, $ECF(\lambda_{\max,EL})$. A more detailed correction would have to take into account the shape of the emission. At the maximum eye sensitivity wavelength $ECF(550\text{ nm}) = 1$.

To single out the material best suited for OLAS application, we define the following figure of merit (FOM):

FOM =

$$[\text{OLED efficiency}/ECF(\lambda_{\max,EL})]/\text{ASE threshold} \quad (3)$$

We decided to use the current efficiency in units of [cd/A] rather than the quantum efficiency (EQE), since the current efficiency depends on various device parameters (e.g., thickness, electrodes, current density, etc.) and is, therefore, in the context of an electrically driven laser a more practical number. The correction of the current efficiency by the ECF yields a number proportional to the electrical quantum efficiency (photons per electron).

The FOMs are listed in Table 2. As a result of the poor ASE thresholds, the materials SY, XB, and XR are not suitable for use in a potential laser diode. Even the famous

MeLPPP and F8BT are of limited use (FOM = 0.20 and 0.07, respectively), due to the poor OLED efficiency. By contrast, our novel green-emitting PSF polymers show FOMs up to 2 orders of magnitude larger (FOM = 8.7 for G5(10)). Within the series of green-emitting polymers, the G5 and G6 materials are preferred over G7, mainly because these materials exhibit lower ASE thresholds. The comparison of cross-linked polymers with chromophores 5 and 6 feature similar FOMs for XG5(15) and XG6(25). Even though XG6(25) has a slightly lower FOM (1.9) compared the XG5(15) (2.6, Table 2), XG6(25) exhibits an important advantage. The overlap of the XG6(25) ASE peak ($\lambda_{\text{ASE}} = 543\text{ nm}$, Figure 1) with the absorption spectrum of TPD radical cations (= positive charge carriers or holes; $\lambda_{\max,abs} = 480\text{ nm}$)⁴⁰ is reduced compared to XG5(15) ($\lambda_{\text{ASE}} = 520.5\text{ nm}$) due to the red-shifted ASE peak (Table 2). This is of crucial importance for future organic laser diodes and amplifiers because the charge absorption of TPD units, included in the X-HTL and in the PSF polymers, can suppress the optical gain.⁴¹ For these reasons, the cross-linkable XG6(25) is the material of choice for the implementation into a thick multilayer device, in which it is sandwiched between a hole-transport and an electron-transport layer that will simultaneously act as optical cladding.⁴²

IV. ASE in a Thick Layer OLED Device

For the realization of an electrically driven organic laser it is necessary to embed the polymeric gain material in an electrically functional device without sacrificing its ASE properties. In the above-described standard OLEDs no ASE could be achieved by optical excitation, because the losses induced by the electrodes exceed the optical gain of the ASE medium by orders of magnitude.²¹ To reduce the losses, the penetration of the optical modes into the electrodes has to be reduced.^{21,29} First attempts are the use of thin electrodes^{20,31} and planar field-effect transistor geometries.⁴³ Rothe et al. achieved optical pumped ASE in an electrically functional thin-film device based on PFO with β -phase as active material.⁴⁴ This result was largely unexpected and is probably related to the presence/formation of the PFO β -phase, which has dramatically different optical properties as compared to the amorphous film.

Our approach is based on the use of thick crosslinkable, hole-transport (X-HTL, 11, Scheme 1) and electron-transport layers (ETL), cladding the XG6(25) layer.⁴¹ Pure polyspirobifluorene, which is obtained by copolymerization of the spirobifluorene–bisboronic acid 1 and the respective dibromo compound (not shown) following

(40) Unpublished results.

(41) Gärtner, C.; Karnutsch, C.; Pflumm, C.; Lemmer, U. *IEEE J. Quantum Electron.* **2007**, *43*, 1006.

(42) Gather, M. C.; Ventsch, F.; Meerholz, K. *Adv. Mater.* **2008**, *20*, 1966.

(43) Nakanotani, H.; Akiyama, S.; Ohnishi, D.; Moriwake, M.; Yahiro, M.; Yoshihara, T.; Tobita, S.; Adachi, C. *Adv. Funct. Mater.* **2007**, *17*, 2328.

(44) Rothe, C.; Galbrecht, F.; Scherf, U.; Monkman, A. *Adv. Mater.* **2007**, *18*, 2137.

(38) Becker, H.; Spreitzer, H.; Kreuder, W.; Kluge, E.; Schenk, H.; Parker, I.; Cao, Y. *Adv. Mater.* **2000**, *12*, 42.

(39) Bolink, H. J.; Cappelli, L.; Coronado, E.; Recalde, I. *Adv. Mater.* **2006**, *18*, 920.

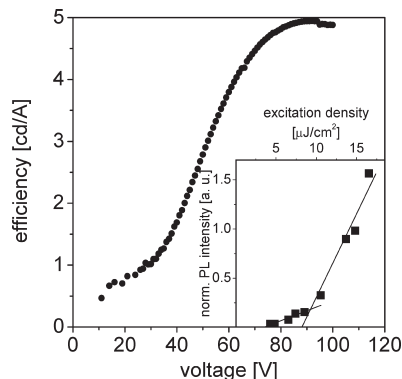


Figure 4. Voltage dependence of the luminous efficiency of the thick multilayer OLED (ITO (150 nm)/PEDOT:PSS (25 nm)/X-HTL (580 nm)/**XG6(25)** (250 nm)/ETL (250 nm)/Ba (4 nm)/Ag (100 nm)). Inset: Intensity of the ASE peak vs excitation density ($E_{th} = 9 \mu\text{J}/\text{cm}^2$).

Scheme 1, is used as ETL. Our thick OLED device has the structure ITO (150 nm)/PEDOT:PSS (20 nm)/X-HTL (580 nm)/**XG6(25)** (250 nm)/ETL (250 nm)/Ba (4 nm)/Ag (100 nm). The thicknesses of the X-HTL and the ETL were chosen to minimize the ASE threshold. Further details about device and optimization of the cladding layers will be described elsewhere.⁴⁵ We achieved a low ASE threshold of the **XG6(25)** in the multilayer OLED ($I_{th} = 9 \mu\text{J}/\text{cm}^2$, Figure 4), that is, comparable to the threshold of a **XG6(25)** single-layer on glass ($I_{th} = 7 \mu\text{J}/\text{cm}^2$, Table 2). The ASE spectrum exhibiting the maximum at 543 nm is shown in Figure 1. Concomitantly, a good luminescence efficiency of 4.9 cd/A is achieved for the device, having an overall thickness of $\sim 1.1 \mu\text{m}$ (Figure 4). This compares favorably to 6.2 cd/A in a common single-layer OLED (Table 2). The normalized EL spectrum (Figure 1) remains unchanged within experimental error for current densities up to $30 \text{ mA}/\text{cm}^2$.

The low losses in the slab-waveguide OLED can be determined from the optical gain at the ASE threshold,

(45) Wallikewitz, B.; Zacharias, P.; Hertel, D.; Meerholz, K. Manuscript in preparation.

(46) Charas, A.; Alves, H.; Alcácer, L.; Morgado, J. *Appl. Phys. Lett.* **2005**, *89*, 143519.

where optical gain and losses are equal. From Figure 3, the optical gain of the PSF copolymers and, thus, the losses in the slab-waveguide OLED can be estimated to $8 \pm 3 \text{ cm}^{-1}$ at $9 \mu\text{J}/\text{cm}^2$.

The low ASE threshold of the **XG6(25)** by optical excitation as well as the good luminescence efficiency by electrical excitation makes this device promising for future electrical driven organic lasers.

V. Conclusions

In conclusion, we have shown that the novel green-emitting PSF polymers presented here are a class of materials that exhibit good OLED performance *and* simultaneously have favorable properties for lasing applications. The ASE thresholds of our polymers ($4.4\text{--}10 \mu\text{J}/\text{cm}^2$) are among the lowest for green-emitting polymers reported so far. They are accompanied by high net gain values of up to 53 cm^{-1} . The gain values are two times higher compared to literature values reported for polyfluorenes.¹⁵ Our findings underline that there is no correlation between OLED and ASE properties and that the cross-linkable polymers presented here with low ASE thresholds and good OLED efficiencies are exceptional.

By using cross-linkable gain media, we were able to fabricate a thick multilayer OLED with low waveguide losses. A low ASE threshold of $9 \mu\text{J}/\text{cm}^2$ is achieved in the fully functional device, that is, comparable to the threshold of a single layer on glass ($7 \mu\text{J}/\text{cm}^2$). Concomitantly, the device exhibits a good luminous efficiency of 4.9 cd/A. The exceptional optical and electrical properties of this device demonstrate its high potential for future electrical driven organic lasers. We are currently working to incorporate resonators in this device.

Acknowledgment. We are indebted to Merck KGaA, Darmstadt and Prof. U. Scherf for providing the polymers used in our study. We would like to thank the BMBF for financial support under the OLAS project FKZ 13N8167.